photonics

MDPI

Article

High-Speed, High-Performance DQPSK Optical Links with Reduced Complexity VDFE Equalizers

Maki Nanou *, Christina (Tanya) Politi, Alexandros Stavdas, Kristina Georgoulakis and George-Othon Glentis

University of Peloponnese, Department of Informatics and Telecommunications, Tripolis, Terma Karaiskaki 22100, Greece; tpoliti@uop.gr (C.P.); astavdas@uop.gr (A.S.); kristina@uop.gr (K.G.); gglentis@uop.gr (G.-O.G.)

* Correspondence: mnanou@uop.gr; Tel.: +30-2710372222

Received: 15 January 2017; Accepted: 24 February 2017; Published: 26 February 2017

Abstract: Optical transmission technologies optimized for optical network segments sensitive to power consumption and cost, comprise modulation formats with direct detection technologies. Specifically, non-return to zero differential quaternary phase shift keying (NRZ-DQPSK) in deployed fiber plants, combined with high-performance, low-complexity electronic equalizers to compensate residual impairments at the receiver end, can be proved as a viable solution for high-performance, high-capacity optical links. Joint processing of the constructive and the destructive signals at the single-ended DQPSK receiver provides improved performance compared to the balanced configuration, however, at the expense of higher hardware requirements, a fact that may not be neglected especially in the case of high-speed optical links. To overcome this bottleneck, the use of partially joint constructive/destructive DQPSK equalization is investigated in this paper. Symbol-by-symbol equalization is performed by means of Volterra decision feedback-type equalizers, driven by a reduced subset of signals selected from the constructive and the destructive ports of the optical detectors. The proposed approach offers a low-complexity alternative for electronic equalization, without sacrificing much of the performance compared to the fully-deployed counterpart. The efficiency of the proposed equalizers is demonstrated by means of computer simulation in a typical optical transmission scenario.

Keywords: advanced optical transmission techniques; digital signal processing; electronic equalization; dispersion compensation

1. Introduction

Due to the rapid evolution of cloud services, traffic demand is growing dramatically every year in every network segment. Especially in core optical networks, this demand necessitates adaptation of high-speed channels in a power efficient and economically viable way. Transporting traffic at high bit rates, such as 100 Gbit/s, may become challenging as various impairments manifest themselves [1]. Combating those impairments is cumbersome and power consuming, hence, the preferred solution choices are not obvious in network segments that are sensitive to cost and power consumption, like in metropolitan area networks [2] and inter-data center networks [3]. Typically, these segments are subject to unpredictable traffic changes and all distortions vary in a nondeterministic way.

Optical transport technologies optimized for such network applications with direct detection (DD) techniques gain an increasing number of supporters due to the adaptivity and low complexity offered by optical and electronic transmission technologies used to compensate for linear and nonlinear impairments [4]. Chromatic dispersion (CD) is the prevailing linear impairment that causes intersymbol interference (ISI) [2]. Distortion compensation techniques have been made readily available with optical and electronic means [5–7]. Optical compensators are usually based on dispersion

compensating fiber (DCF) placed along the optical transmission system, while electronic ones are usually based on equalizers. Optical compensating techniques are rigid as far as the amount of the CD they mitigate implying that its value is known in advance. Electronic equalizers [5,8], on the other hand, are utilized adjustably after signal detection and can additionally compensate part of the PMD [6]. Equalization methods can be performed by a maximum likelihood sequence estimation (MLSE) method [6] or on the use of non-linear decision feedback filters for mitigating ISI in optical communication systems. Equalization methods based on recursive Volterra nonlinear filters have been proposed [7,9], noting however, that the use of Volterra equalizers still becomes cumbersome when the ISI extends more than a few symbols.

In high data rate systems, signal distortions caused by intersymbol interference increase proportionally to the square of the data rate, hence, the performance of the transmission system is very sensitive to the possible residual dispersion at the receiver. Optical dispersion compensation can only compensate for specific values of chromatic dispersion, however, in dynamic multi-channel network segments dispersion is not always known in advance. As discussed in [2] optical transmission systems can benefit from a combination of rigid DCF with adaptive equalization at the receiver where residual dispersion is adjustably compensated after signal detection.

In this paper, we investigate the performance of the conventional non-return to zero differential quaternary phase shift keying (NRZ-DQPSK) optical link that comprises an optical channel with standard single mode and dispersion compensating fiber and various receiver configurations that combine single-ended receivers and joint reduced complexity Volterra-type equalizers [2,10,11]. For the first time, to our knowledge, the scope of the investigation takes advantage of the linear dependency among the electrical signals (constructive/destructive and in-phase/quadrature) at the receiver side, to further reduce the complexity of proposed equalizers, allowing for numerically sound and viable implementation configurations. The proposed partially-joint single-ended digital equalization schemes for the DQPSK signaling utilize a triplet out of the quartet of electrical signals (constructive/destructive and in-phase/quadrature) available at the single ended receiver, for equalization, and eventually the detection of the transmitted bit streams. As a result a 25% reduction of the computational cost compared to the fully-deployed joint counterpart is achieved. As the hardware implementation circuitry of a digital equalizer is proportional to the computational complexity and the memory requirements [2,10,12], the proposed approach offers reduced cost solutions that can be viably applied for the equalization of high-speed, high-performance optical transmission systems. A comparative study of the performance of the proposed equalization schemes is performed by means of computer simulations, using a typical 40 Gb/s optical transmission setup.

2. DQPSK Equalization

DQPSK is a four-level modulation format initially introduced to overcome spectral efficiency limitations of direct detection binary modulation formats [1]. Recently, DQPSK has been revisited together with other direct detection techniques for cost efficiency [13] or nonlinearity mitigation [14]. Today, processing the signal electronically at symbol rate speeds is very typical in coherent optical transponders, however, in applications restricted by cost, direct detection is revisited [15–17] and DQPSK is a very important candidate [2]. Let $I_1(n) \in \{0,1\}$ and $I_2(n) \in \{0,1\}$ represent the encoded transmitted sequences of the I and Q channels, which are encoded and modulated using a standard DQPSK transmitter setup (Figure 1). A typical optical communication link consists of numerous identical fiber spans where part of the accumulated dispersion in the single mode fiber (SMF) is compensated by means of DCF and losses by optical amplifiers. At the receiver side, after optical bandpass filtering, the signal is demodulated by means of two separate Mach Zehnder delay interferometers (MZDI). Each arm of the MZDI has a phase shift of $\pi/4$ (in-phase component) and $-\pi/4$ (quadrature component). Subsequently, each output of the MZDI devices is detected by a photodiode and is filtered by an electrical low-pass filter (ELPF), producing in this way a set of constructive and destructive signals for the in-phase, as well as for the quadrature component, denoted here by $I_c(t)$, $I_d(t)$, $Q_c(t)$, and $Q_d(t)$, respectively [18]. Although any pair of the combination $\{I_c(t),I_d(t)\} \times \{Q_c(t),Q_d(t)\}$

may be utilized for the detection of the transmitted sequences, a scheme based on the differential output $I(t) = I_c(t) - I_d(t)$ and $Q(t) = Q_c(t) - Q_d(t)$, known as 'balanced detection', is usually used instead, offering in this case a 3 dB OSNR gain compared to the former approach.

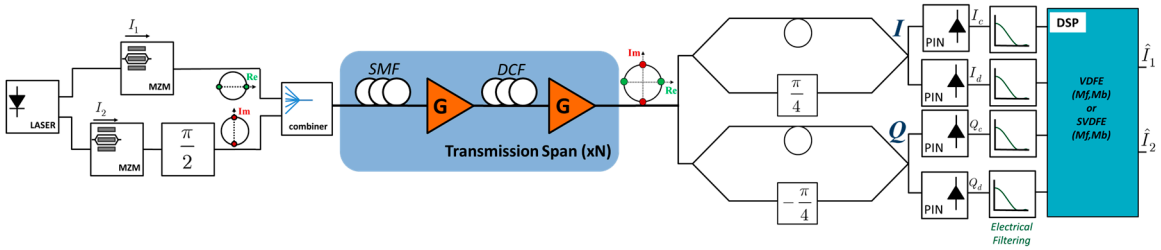

Figure 1. Block diagram of a NRZ-DQPSK set exhibiting N transmission spans and a single wavelength transmitter together with a typical single-ended receiver.

Electronic equalization is usually applied for the suppression of either all, or a part (residual) of the distortions introduced by the fiber. In the case when the DQPSK receiver is implemented by means of balanced detection, the equalization methods are referred to as 'balanced DQPSK equalization'. However, it has been demonstrated that the joint use of all the signals available at the receiver for equalization, provides improved results compared to those obtained if the differential output signals are used instead, for sequence, as well as for symbol-by-symbol equalization [9,19]. The latter approach is known as 'joint DQPSK equalization'.

Symbol-by-symbol electronic equalization of direct detection optical transmission by means of recursive Volterra nonlinear filters has drawn significant attention in the past, for NRZ, DPSK, and DQPSK signaling. The feasibility of the implementation of those methods on FPGA (Field-Programmable Gate Array) circuitry has recently been demonstrated [2,12,20], for rates up to 40 Gb/s. Due to the joint constructive/destructive processing, four signals are available as input to the equalizer. Further signal diversity is achieved by fractionally spaced sampling, as in this case the performance of the electronic equalizers becomes less sensitive to the sampling phase of the receiver [21]. We here adopt half rate spaced sampling, $T_s/2$, where T_s is the symbol period. Thus, after digital to analog conversion (D2A), eight signals (depicted on Figure 2a) are eventually fed to the feed-forward part of the equalizer, namely:

$$\begin{array}{c} y_{1,1}(n) \triangleq I_c(nT_s), y_{2,1}(n) \triangleq I_c(nT_s + T/2) \\ y_{1,2}(n) \triangleq I_d(nT_s), y_{2,2}(n) \triangleq I_d(nT_s + T/2) \\ y_{1,3}(n) \triangleq Q_c(nT_s), y_{2,3}(n) \triangleq Q_c(nT_s + T/2) \\ y_{1,4}(n) \triangleq Q_d(nT_s), y_{2,4}(n) \triangleq Q_d(nT_s + T/2) \end{array} \quad (1)$$

Following [19], a symbol-by-symbol, joint DQPSK Volterra decision feedback (VDFE) equalizer, is described as ($l = 1, 2$):

$$u_l(n) = \sum_{i=1}^{2}\sum_{k=1}^{4}\sum_{m=0}^{M_f-1} f_{i,m}^{k,l} y_{i,k}(n-m) + \sum_{i=1}^{2}\sum_{k=1}^{4}\sum_{m_1=1}^{M_f-1}\sum_{m_2=m_1}^{M_f-1} f_{i,m_1,m_2}^{k,l} y_{i,k}(n-m_1) y_{i,k}(n-m_2) + \sum_{i=1}^{2}\sum_{m_1=1}^{M_b}\sum_{m_2=m_1}^{M_b} b_{i,m_1,m_2}^{l} \hat{I}_i(n-m_1)\hat{I}_i(n-m_2) \quad (2)$$

where $u_1(n)$ and $u_2(n)$ are the output signals of equalizer for the in-phase and quadrature part, respectively. Parameters designated by symbol f correspond to the feed-forward (FF) part of the equalizer which compensates for the precursor distortions. Parameters designated by symbol b correspond to the feedback (FB) part of the equalizer which compensates for the post cursor distortions correspondingly. Integers M_f and M_b represent the memory of the FF and the FB part of the equalizer, respectively, and are both related to the amount of distortions that affect the transmission.

Signals $\hat{I}_1(n) \triangleq D[u_1(n)]$ and $\hat{I}_2(n) \triangleq D[u_2(n)]$ represent the recovered in-phase and quadrature bit streams, with D denoting the decision device, as it is explained also in [7,9] and [22]. Hence, the VDFE equalizer described by Equation (2), hereafter will be denoted as VDFE[M_f,M_b], and its structure is summarized in Figure 2b.

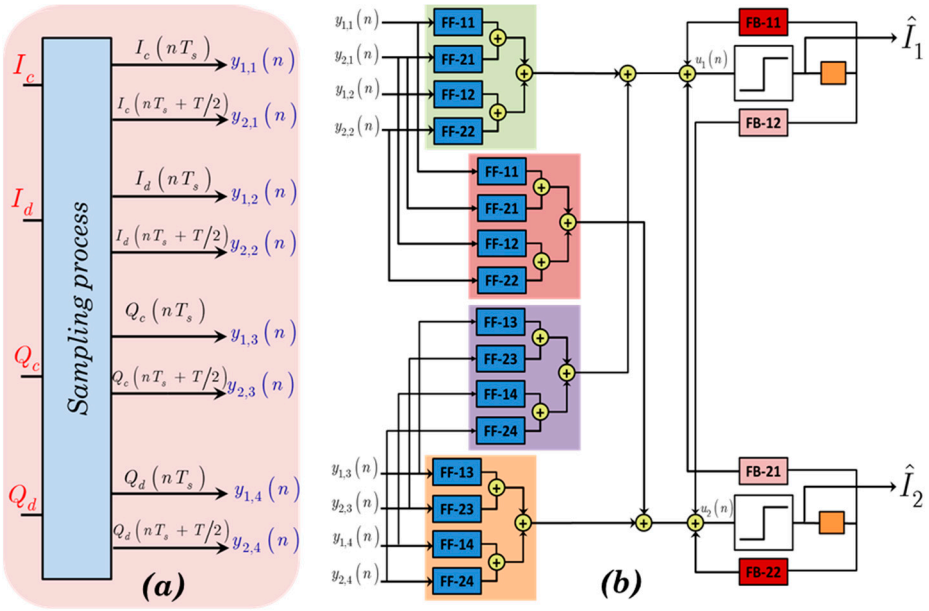

Figure 2. (**a**) Schematic illustration of utilized signals sampled with fractional spacing f and (**b**) signal flow graph or the DQPSK single-ended joint VDFE equalizer.

The mathematical formulae that describes the VDFE can be expressed in a linear regression form as $u_l(n) = \theta_l^T \varphi_M(n),\ l = 1,2$ where $\varphi_M(n)$ is a vector that depends on the input signals and on the recovered bit streams, $\theta_l,\ l = 1,2$ represents the vectors that carries the equalizer coefficients for the in-phase and the quadrature part of the equalizer, with T denoting the matrix transpose. Integer M denotes the number of coefficients for each part of the equalizer. It provides a metric of complexity of the implementation of the recursive scheme, as the number of multiplications and additions required for the computation of $u_1(n)$ and $u_2(n)$ is $C = 2\,M$, in our case given by:

$$C_{VDFE(M_f,M_b)} = 16M_f + 8M_f\left(M_f + 1\right) + 2M_b(M_b + 1) \tag{3}$$

The equalizer coefficients $\theta_l,\ l = 1,2$ are estimated by minimizing a properly chosen cost function between the output signals and a desired response signal [22]. The least squares (LS) estimator is perhaps the most popular design approach, where the parameters sought are estimated minimizing the sum of the squared error between the output of the equalizer and a set of N training data, $I_1(0), I_1(1), \ldots, I_1(\mathrm{N}-1)$ and $I_2(0), I_2(1), \ldots, I_2(\mathrm{N}-1)$, in our case. The optimum parameter vectors $\theta_l,\ l = 1,2$ correspond to the solution of a linear system of equations, the so called 'normal equations', which is obtained either explicitly by means of a direct system solver, or implicitly engaging an iterative or a time recursive estimation scheme. In the case of time varying distortions, the estimated values may be updated either periodically or on a sample-by-sample basis, blindly working in a decision-directed mode.

A significant reduction in the computational complexity of the equalization devices in DQPSK signaling may be obtained by processing the differential signals using balanced detection at the receiver. The formulation of the pertinent equalization schemes follow the guideline described above for the case of joint constructive/destructive processing, noting however, that the signal diversity at the receiver is limited to half of that in the former case, as instead of eight, four signals are now

available for digital processing, namely $y_{1,1}(n) \triangleq I(nT_s)$, $y_{2,1}(n) \triangleq I(nT_s + T_s/2)$, $y_{1,2}(n) \triangleq Q(nT_s)$, $y_{2,2}(n) \triangleq Q(nT_s + T_s/2)$. As a consequence, the complexity of the corresponding balanced DQPSK equalizers are reduced to about half of that required for the joint processing case, however, at the expense of a significant deterioration in the attained performance [2,21].

3. Proposed Partially-Joint Single-Ended DQPSK Equalization

Boosting the performance while keeping the cost low is a challenging task in the design of reliable optical links. Low-complexity balanced DQPSK equalization demonstrates poor performance compared to the joint single-ended alternatives [2]. Motivated by former studies concerning the performance of the balanced receivers in DPSK and in DQPSK signaling [19,23,24], we proposed the use of a low complexity, partially-joint single-ended equalization scheme, using a subset of the signals available at the receiver, described by one of the possible combinations (I_c, Q_c, Q_d), (I_d, Q_c, Q_d), (I_c, I_d, Q_c), and (I_c, I_d, Q_d). Due to fractionally-spaced sampling, each triplet corresponds to six signals that are digitally processed by the pertinent equalizer. The proposed three-port partially-joint single-ended VDFE equalizers, hereafter denoted by the ignored port, e.g., VDFE[M_f, M_b]-I_x or VDFE[M_f, M_b]-Q_x, offer approximately a 25% reduction in the required circuitry, compared to the full joint processing counterpart. As it will be demonstrated in Section 4, the proposed approach offers a low complexity alternative for electronic equalization, without sacrificing much of the performance if any at all, compared to the fully deployed counterpart. In order to complete the investigation of partially joint equalizer counterparts, also two port partially joint single ended VDFE equalizers are compared to the balanced receiver VDFE equalizers. All of the aforementioned equalization/receiver-related configurations are depicted in Figure 3.

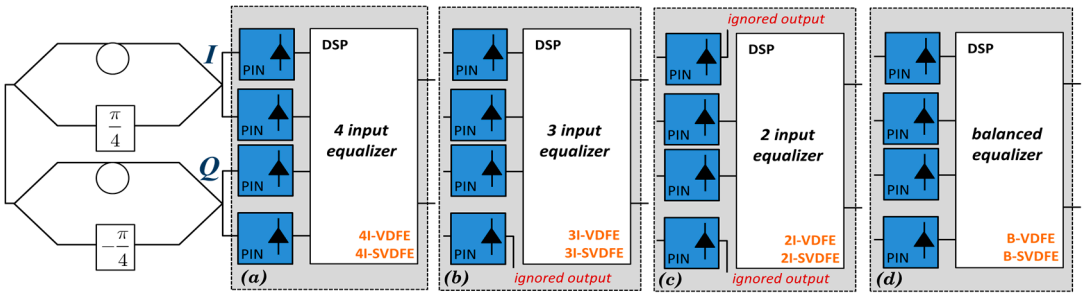

Figure 3. Schematic explanation of different equalizer configurations depending on the receiver type (single-ended or balanced) and number of inputs engaged in the equalization process: (**a**) four-input joint single-ended equalization; (**b**) three-input partially-joint single-ended equalization; (**c**) two-input partially-joint single-ended equalization; and (**d**) balanced equalization.

Let us consider that the signals processed are given by the triplet (I_c, Q_c, Q_d), i.e., the destructive port of I channel has been ignored, hence, the six signals (depicted on Figure 4a) fed to the feed-forward part of the equalizer are:

$$\begin{array}{c} y_{1,1}(n) \triangleq I_c(nT_s), y_{2,1}(n) \triangleq I_c(nT_s + T/2) \\ y_{1,2}(n) \triangleq Q_c(nT_s), y_{2,2}(n) \triangleq Q_c(nT_s + T/2) \\ y_{1,3}(n) \triangleq Q_d(nT_s), y_{2,3}(n) \triangleq Q_d(nT_s + T/2) \end{array} \tag{4}$$

Now the three-port partially-joint single ended VDFE equalizers VDFE[M_f,M_b]-I_d (presented in Figure 4b) is described as: ($l = 1, 2$).

$$\begin{array}{c} u_l(n) = \sum_{i=1}^{2}\sum_{k=1}^{3}\sum_{m=0}^{M_f-1} f_{i,m}^{k,l} y_{i,k}(n-m) + \sum_{i=1}^{2}\sum_{k=1}^{3}\sum_{m_1=1}^{M_f-1}\sum_{m_2=m_1}^{M_f-1} f_{i,m_1,m_2}^{k,l} y_{i,k}(n-m_1) y_{i,k}(n-m_2) + \\ \sum_{i=1}^{2}\sum_{m_1=1}^{M_b}\sum_{m_2=m_1}^{M_b} b_{i,m_1,m_2}^{l} \hat{I}_i(n-m_1)\hat{I}_i(n-m_2) \end{array} \tag{5}$$

The three remaining cases are treated in a similar way. A metric of complexity of the implementation of the recursive scheme, is $C = 2M$, given by:

$$C_{VDFE(M_f,M_b)} = 12M_f + 6M_f\left(M_f + 1\right) + 2M_b(M_b + 1) \tag{6}$$

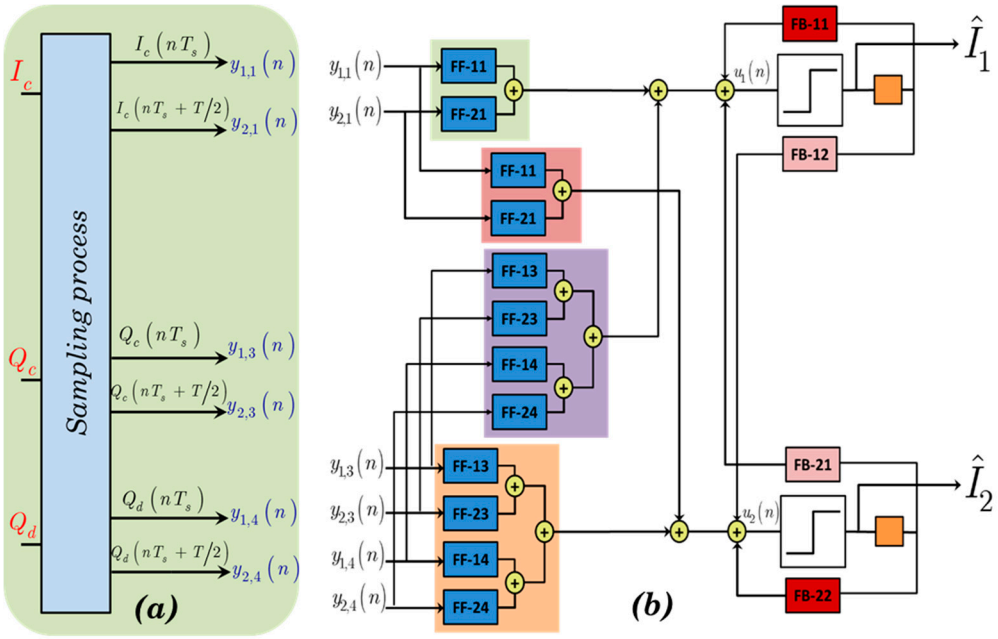

Figure 4. (**a**) Schematic illustration of utilized signals and (**b**) signal flow graph for the proposed partially-joint single-ended DQPSK VDFE[M_f,M_b]-I_d.

Despite its high efficiency in combating the introduced distortion, VDFE in DQPSK exhibits quadratic computational complexity with respect to the ISI size. The increased hardware requirements raise a barrier in the deployment of such device in low-cost, high-speed optical links. To alleviate the complexity issues inherently introduced in the VDFE, reduced complexity counterparts has recently been introduced [11], resorting to pruning techniques for the reduction of the size of the pertinent Volterra kernels, suppressing that part of the Volterra kernel that has a marginal contribution in the overall performance. The resulting pruned VDFE (PVDFE) equalizers, compared to the full-term design, is more tractable from an implementation point of view, leading to significant computational complexity savings, without sacrificing much of the performance compared to the fully-deployed counterpart.

A low complexity alternative of proposed three port partially joint single ended VDFE, is a degenerated form of PVDFE, the so called skimmed VDFE (SVDFE) [10], where extreme pruning is applied to the feed-forward Volterra kernels, keeping only the coefficients that correspond to the diagonal of the full sized counterpart. VDFE employing skimmed Volterra kernels in place of the full-sized counterparts, have been proposed as a viable solution in high-speed, low-cost implementation for the equalization of OOK keying signaling, as well as for the DQPSK modulation, operating at bit rates as high as 40 Gb/s [2,10,12,20]. Assuming the same example of Equation (4), let the signals processed given by the triplet (I_c, Q_c, Q_d), i.e., the destructive port of the I channel, be ignored. Now the three-port partially-joint single-ended SVDFE equalizers VDFE[M_f,M_b]-I_d is described as: ($l = 1, 2$).

$$\begin{aligned} u_l(n) = &\sum_{i=1}^{2}\sum_{k=1}^{3}\sum_{m=0}^{M_f-1} f_{i,m}^{k,l} y_{i,k}(n-m) + \sum_{i=1}^{2}\sum_{k=1}^{3}\sum_{m_1=1}^{M_f-1} f_{i,m_1,m_1}^{k,l} y_{i,k}^2(n-m_1) + \\ &\sum_{i=1}^{2}\sum_{m_1=1}^{M_b}\sum_{m_2=m_1}^{M_b} b_{i,m_1,m_2}^{l} \hat{I}_i(n-m_1)\hat{I}_i(n-m_2) \end{aligned} \tag{7}$$

The cases of all three-port partially-joint single-ended skimmed VDFE equalizer, (SVDFE[M_f,M_b]-I_x or SVDFE[M_f,M_b]-Q_x) are treated similarly. In Figure 5 the differences in structure of the feed-forward part between VDFE (Figure 5a) and SVDFE (Figure 5b) are depicted. While, in this particular block diagram the pruning procedure is presented only for one of the received signals it should be noted that the same technique implies for every different input signal.

The computational complexity for the estimation of $u_1(n)$ and $u_2(n)$ is now reduced to:

$$C_{SVDFE(M_f,M_b)} = 24M_f + 2M_b(M_b + 1) \tag{8}$$

Compared to the complexity requirements of the fully-deployed counterpart (Equation (2)), a significant reduction is achieved, as in the latter case the computational requirement depends linearly on M_f, noting that the contribution of the last term in the summation is rather marginal as $\hat{I}_1(n)$ and $\hat{I}_2(n)$ represent binary digits.

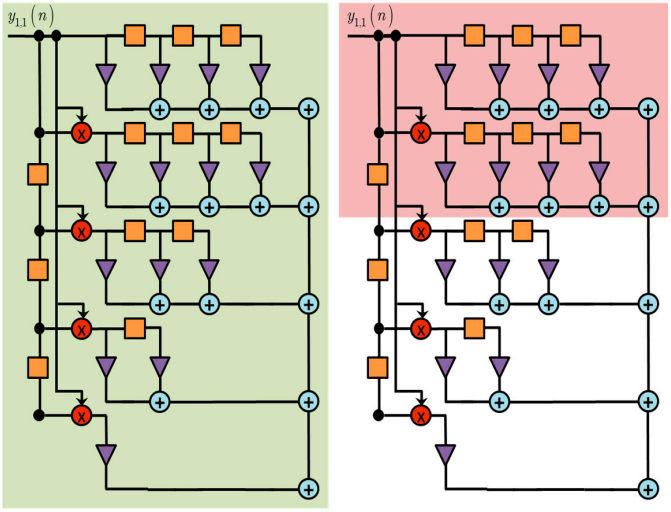

Figure 5. The differences in FF part structure for an equalizer of M_f = 4 between (**a**) VDFE and (**b**) SVDFE.

Apart from the complexity reduction, the proposed partially-joint constructive/destructive equalization scheme offers better numerical behavior compared to the full counterpart. The use of all four signals $I_c(t)$, $I_d(t)$, $Q_c(t)$, and $Q_d(t)$, available at the DQPSK receiver, improves performance by maximizing the signal diversity. MLSE equalizers certainly benefit from this approach, however, in the case of symbol by symbol equalizers, such as DFE and VDFE, some extra attention is required. Following the low-pass equivalent description of a DQPSK link [24], we notice that in the case of ideal identical noise free photodetectors, the four electrical signals available at the receiver, $I_c(t)$, $I_d(t)$, $Q_c(t)$, and $Q_d(t)$ are linearly dependent, as it can be easily shown that $I_c(t) + I_d(t) - Q_c(t) - Q_d(t) = 0$. In a realistic situation, the presence of noise at the receiver results in (marginally) linear independence, as $I_c(t) + I_d(t) - Q_c(t) - Q_d(t) = n(t)$, with $n(t)$ denoting the contribution of the noise signals from all four photodiodes. Noting that the coefficients of the VDFE equalizer (Equation (2)) are estimated by the solution of a linear system of equations either implicitly or explicitly, the condition number of the associated matrix which is formulated using the available signals (Equations (1)), is of crucial importance concerning the numerical accuracy of the estimated output [22]. In the undesired situation when $n(t)$ is much weaker than the remaining signals, the numerical behavior of the algorithm utilized for the estimation of the equalizer parameters (also known as the linear system solver) will deteriorate, resulting in severe ill-conditioning. A remedy to this problem is to resort to the use of proper regularization, such as the diagonal loading method, requiring extra effort for the handling of this overhead. On the contrary, the proposed partially-joint VDFE and its derivatives,

do not suffer from such an effect, as three out of four electrical signals $I_c(t)$, $I_d(t)$, $Q_c(t)$, and $Q_d(t)$, are engaged only. Simulation results indicated that the calculated condition number of the matrices involved into the estimation of the parameters of the equalizers (linear system of equations), vary from 10^6 up to 10^{10} in the case of fully-joint constructive/destructive equalization. This figure is reduced to 10^3 in the case of partially-joint equalization.

4. Optical Layer Simulation

As shown in previous work [2,12,20,25] the amount of dispersion that an equalizer can compensate is directly related to both the memory of the FF$\left(M_f\right)$ and FB(M_b) filters. As the values of M_f and M_b increase, the performance of the equalizer in compensating chromatic dispersion improves. In Figure 6 the performance of VDFE and SVDFE equalizers for different sets of [M_f,M_b] are presented accompanied with the total number of coefficients used for each case. It has become evident that, for both VDFE and SVDFE, large numbers of M_f and M_b (e.g., [13,7] and [11,6]) result in a dramatic increase of the number of coefficients but does not result in a notable increase in performance compared to the equalizers with smaller values of [M_f,M_b] (e.g., [9,5]).

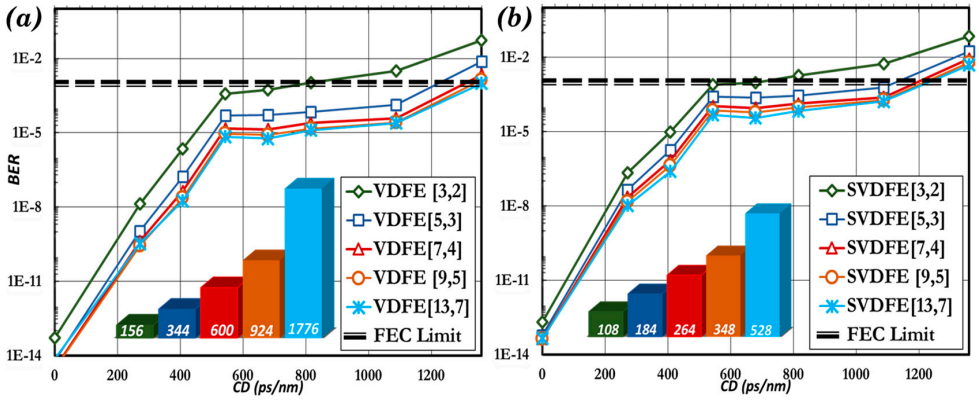

Figure 6. Performance of (**a**) VDFE; (**b**) SVDFE, and the number of coefficients for each case.

When electronic equalization is used in conjunction with optical compensation, as in the cases suggested here, the memory of the FF and the FB part of VDFE type equalizers does not need to be high, and VDFE[M_f,M_b] with [M_f,M_b] = [5,3] and [9,5] are sufficient [2]. As a result, the performance of the optical communications system can be significantly improved, in the sense of reaching an extended transmission distance, or by improving the bit error rate (BER) of the received signal. In order to provide the whole picture about the suggested electronic equalization solution, their efficiency is evaluated by means of two different numerical modeling sets of an optical link that operates at 40 Gb/s using a DQPSK modulation format (Figure 7).

The first modeling setup (Figure 7a), referred hereafter as noise loading scenario, utilizes the OSNR metric to evaluate the performance of the optical transmission system, which can be defined as:

$$OSNR|_{dB} = 10\log_{10}\left(\frac{P_{signal}}{P_{noise}}\right) \quad (9)$$

Any variation of the OSNR subsequently leads to variation in the quality and, hence, the BER value of the detected signal. Thus, the OSNR requirement to achieve a specific BER (referred as rOSNR) can provide a figure of merit for the performance of a system. The performance of each receiver/equalizer combination in an optical transmission system is evaluated through modelling of an uncompensated link, which consists of a single mode fiber, without utilizing any optical dispersion compensating module. While SMF is considered lossless, the total accumulated dispersion varies from 100 ps/nm to 1500 ps/nm. The OSNR value varies by adding Gaussian-distributed optical white noise

before the optical receiver emulating various levels of amplified spontaneous emission (ASE) at the receiver end, while a bandwidth of B_0 = 12.5 GHz is used to calculate the OSNR value. On the receiver side a bandpass optical filter with 40 GHz bandwidth is used to reduce the ASE noise that enters the MZDI and subsequently the PIN.

For the second setup (Figure 7b), a multi-span transmission link is numerically simulated, which consists of eight identical spans (8 × 100 km) where a partial compensation of the accumulated dispersion is performed by the means of DCF, while the residual dispersion is handled by the electronic equalizer. A metric that defines the amount of the optical dispersion compensation is introduced, called the optical compensation ratio, hereafter denoted as OCR, and varies from 80% to 99% of the total accumulated dispersion. For the simulations, each span consists of an SMF with D = 17 ps/nm/km, attenuation parameter of a = 0.2 dB/km, and a DCF with a dispersion parameter D = −85 ps/nm/km and a = 0.5 dB/km. The fiber model uses the split step Fourier method in order to solve the nonlinear Schroedinger (NLS) equation, taking into account fiber nonlinearities and the nonlinear coefficient n_2 has a value of 2.6 × 10^{-20} m^2/W while PMD is not considered. Moreover, a two-stage amplification process is used, modelled by two separate amplifiers with a 5 dB noise figure, each one of them utilized to compensate either the SMF or the DCF losses. For both of the aforementioned set up scenarios the transmitter/receiver configuration is considered identical. At the transmitter side, the DQPSK signal is generated via two different MZM (one per channel) which operate in a push-pull mode and have an extinction ratio of 35 dB each. In terms of electrical filtering two low pass third-order Bessel filters are used with a cut-off frequency of 40 GHz. For the PRBS, the modified Wichman-Hill generator [26] is used with a mark probability of 0.5. The transmitter operates at the optical frequency of 193.1 THz with 0 dBm output power. On the receiver side, an optical filter of 40 GHz bandwidth with a third-order Gaussian frequency response is utilized. In order to demodulate the DQPSK signal, two different MZDI are used. After each MZDI output port a photodiode of 1 A/W responsivity and a fourth-order Bessel frequency response electrical filter is used in order detect the optical signal. The input power is chosen to be well above the noise limit and below the nonlinear limit of the system. It is noted, however, that in a realistic system where WDM is used and the number of channels increases, the optical power and crosstalk will be dominant, and the parameters will be re-evaluated.

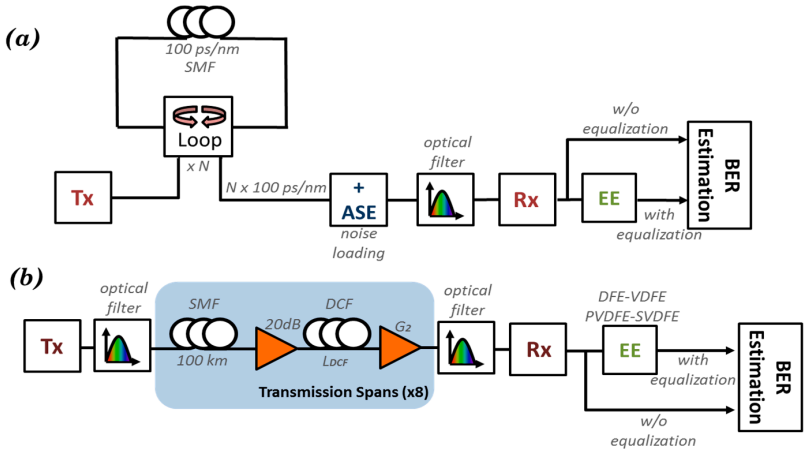

Figure 7. Simulation generic setup for (**a**) a noise-loading technique and (**b**) multi-span scenarios with eight spans.

The numerical simulations are performed by the means of Virtual Photonics Inc. software (VPI Transmission Maker) and approximately 10^6 bits are used for BER computation, in order to achieve higher accuracy.

The results of the noise loading scenario of each equalizer (SVDFE and VDFE) are depicted in Figure 8 for both $[M_f,M_b]$ = [5,3] and [9,5]. The specific sets of $[M_f,M_b]$ exhibit sufficient compensation capability, and the equalizer complexity makes it feasible in terms of implementation [2].

The required OSNR with respect to accumulated dispersion is plotted for all equalizer cases discussed in Sections 2 and 3, along with the performance of the optical system when dispersion compensation is performed only by optical means (without the equalizer case). Apart from the single-ended joint version, where all four output ports are utilized (denoted in figures as 4I), each equalizer is compared with all three partially-joint input counterparts (denoted in figures as 3I). Those partially-joint single-ended configurations differentiate themselves according to the number of ports (e.g., 3I three input) and the specified disregarded input port (e.g., 3I-VDFE[5,3]-I_d). Depending on the output that is not utilized, every configuration exhibits slightly different performance. All of the different configurations seem to offer a significant improvement in the performance of the system under investigation, compared to the case where no electronic equalization is used (without equalizer). Assuming that the rOSNR should be approximately 18 dB, 4I equalization schemes seem to increase the amount of tolerable CD up to 1200 ps/nm (SVDFE[5,3]) and 1325 ps/nm (VDFE[5,3]), corresponding to 70 km and 80 km of uncompensated fiber, respectively. The increase of the tolerable amount of CD is even greater when equalizers with [M_f,M_b] = [9,5] are deployed. When no equalization is used the tolerable amount of chromatic dispersion reaches up to 300 ps/nm (corresponding to 17 km of uncompensated CD), hence, utilizing equalization can extend the uncompensated distance approximately up to 60–80 km (depending on the equalizer type and the set of [M_f,M_b]). This improvement on the CD tolerance of the system comes at the expense of increased required OSNR, since as the amount of residual dispersion increases, the value of rOSNR increase also. The rOSNR deterioration is saturated at 600 ps/nm, indicating that the equalizer is slowly reaching its full potential in terms of alleviating the residual CD. Although every equalizer succeeds in ensuring the proper operation of the system (by achieving a BER of 10^{-3}), for a certain amount of additional dispersion there is point where the increase in the required OSNR becomes dramatic and the performance is deteriorated. From Figure 8 it becomes evident that although the best efficiency is achieved by the four-input joint single-ended VDFE and SVDFE, all three-input partially-joint alternatives exhibit marginal differences in performance.

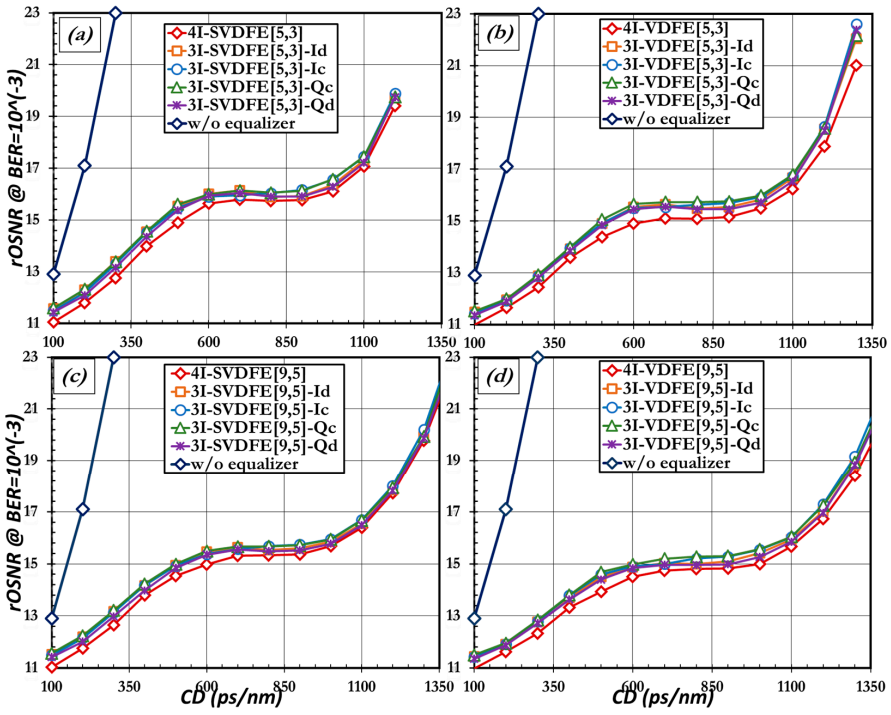

Figure 8. Required OSNR performance of comparison between the joint single-ended configurations (4I-) and the partially-joint three-input ones (3I) for the cases of (**a**) SVDFE[5,3]; (**b**) VDFE[9,5], (**c**) SVDFE[9,5]; and (**d**) VDFE[9,5].

All of the aforementioned conclusions can also be verified by the results that are derived by the numerical modeling of the multi-span transmission system shown in Figure 7b and are depicted in summary in Figure 9. The OSNR of this specific transmission system is approximately 18 dB measured at a bandwidth of 12.5 GHz. In this case the BER of the signal received after equalization is estimated and presented with respect to the variable amount of chromatic dispersion that emerges due to the partial optical compensation (OCR = 80%–99%). These performances are presented along with the case where no electronic equalization is used (without equalizer) and the FEC (Forward Error Correction) limit = 10^{-3}.

Nonetheless, apart from the minor differences in the performance of all of the possible candidates, one can conclude that the solution of utilizing an equalization scheme that ignores branch Q_d can offer the best trade-off between complexity and efficiency. On the contrary, all equalizers that ignore Q_c output seems to experience the worst performance although its difference in efficiency is still marginal. Similarly, regarding the I channel of information, ignoring the I_d port instead of the I_c port presents better performance. This feature can be justified by noting that the constructive output port is resembles a duobinary (DB) signal, while the destructive output port resembles an alternating-mark-inversion (AMI) signal [27,28]. The intrinsic high tolerance of the DB modulation format in chromatic dispersion originates from its narrow spectrum [29] and can explain the better performance of every equalizer when the constructive, rather than the destructive, port (of each channel) is maintained to undergo the process of equalization [30].

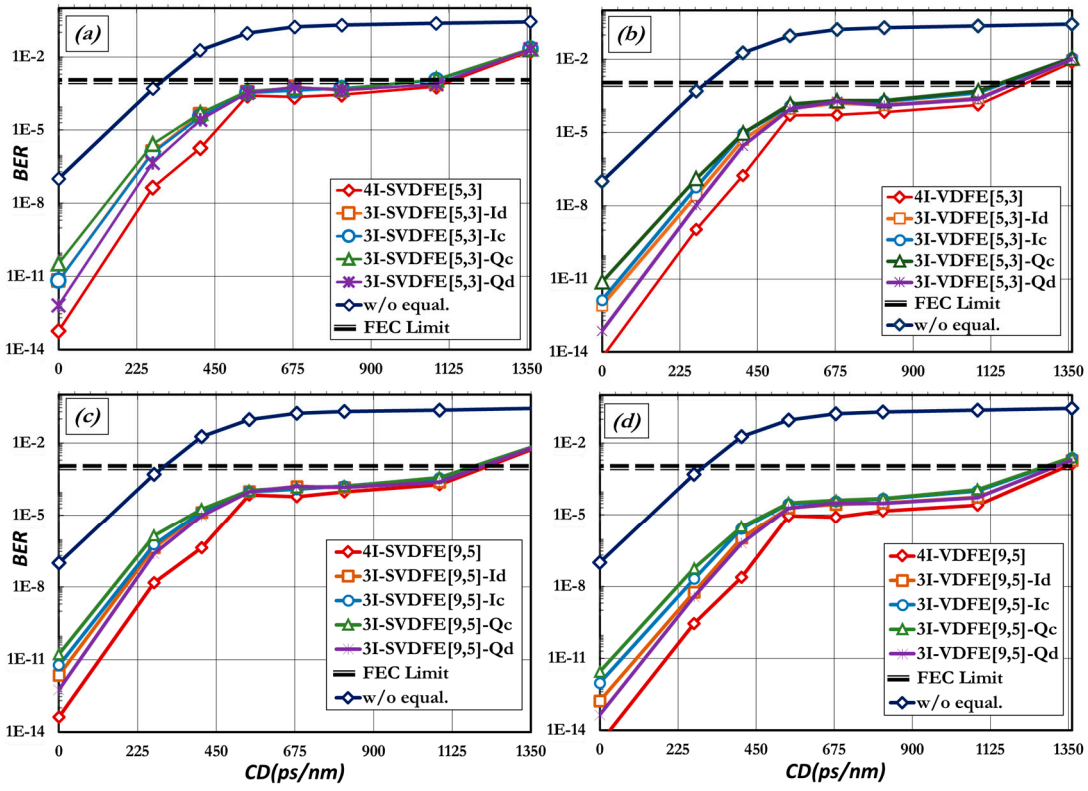

Figure 9. Estimated BER of optical links that utilize (**a**) SVDFE[5,3]; (**b**) VDFE[5,3]; (**c**) SVDFE[9,5]; and (**d**) VDFE[9,5] equalizers depending on the ignored input signal (I_c ,I_d, Q_c, Q_d). 4*I* and 3*I* denote the number of inputs.

Since ignoring the destructive output port of each channel (*I* or *Q*) seems to be the most efficient solution among the partially joint configurations in terms of alleviating the CD effect, it becomes of interest to investigate the performance of a degenerated equalizer in which the destructive outputs of both *I* and *Q* channel are ignored, resulting in a two-input partially-joint equalizer (denoted here after

as 2*I*). The two-input partially-joint equalizer offers the lowest complexity among all of the different single–ended receiver configurations. In order to provide a fair comparison in terms of efficiency, the performance of the two-input partially-joint equalizer is presented along with the performance of the balanced receiver/equalizer combination [2], considering that the complexity of the configurations are also comparable.

In Figure 10 the estimated BER of the two-input configuration for every equalizer is depicted, along with the performance of balanced configuration, in respect to variable amounts of residual dispersion. The complexities of balanced and two-input equalization are comparable and the performance of the balanced scheme surpasses the one offered by the two-input partially-joint single-ended configuration for every type of equalizer (SVDFE, VDFE) and for all sets of $[M_f,M_b]$. However, the superiority of balanced equalization becomes more evident as the values of M_f and M_b increase. It should be highlighted that the balanced VDFE[9,5] (i.e., B-VDFE[9,5]) is able to alleviate up to 630 ps/nm of residual dispersion and, thus, almost doubles the dispersion tolerance of the optical system, compared to the case where the compensation is performed only with optical means, whereas the equivalent two-input partially-joint equalizer (2I-VDFE[9,5]-IdQd) that carries the same complexity can reach dispersion tolerance values up to ~500 ps/nm. The performances of four-input and three-input equalizers exceed, by far, those offered by the two-input partially-joint and balanced equalizers and are presented here only for completeness.

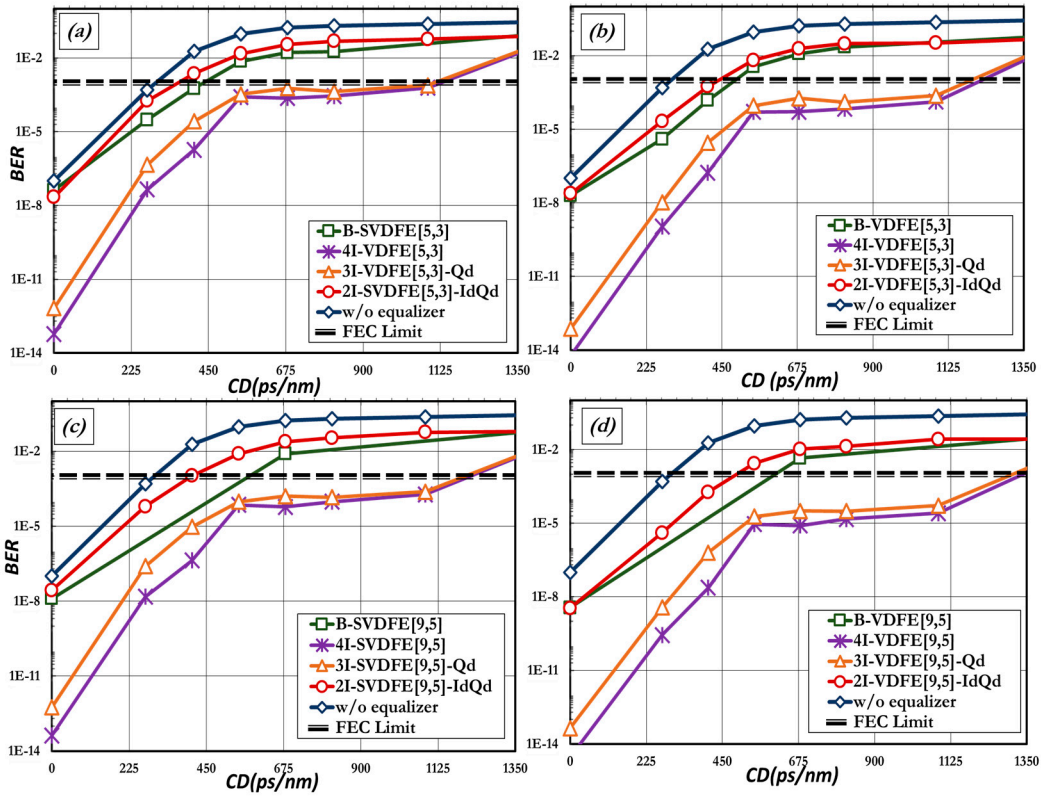

Figure 10. Estimated BER of optical links that utilize (**a**) SVDFE[5,3]; (**b**) VDFE[5,3]; (**c**) SVDFE[9,5] and (**d**) VDFE[9,5] for 2I-, 3I, and balanced equalization.

Disregarding inputs from the equalization process proved to be exceptionally efficient when compared against the performance of four-input joint single-ended equalizers on one hand, and low complexity balanced receiver equalizers on the other. The first case exhibits high performance, high complexity, and questionable numerical accuracy. High complexity is dictated by the number of filters that are used. Furthermore numerical accuracy is compromised by the linear dependency of the optical inputs that leads to high condition numbers in the equalization process. The balanced case exhibits

low performance, but very low complexity and cost. In this paper, starting from the requirements for low-complexity, high-performance equalizers, the effect of reducing the number of single-ended ports in the equalization process is investigated with exceptional results. Due to the nature of DQPSK, when one of the destructive ports is not utilized in the equalization process, even low-complexity VDFE equalizers manage to compensate for residual dispersion. However, it has been proved that when it comes to ignoring more than one input at the same time (i.e., both destructive input ports) the performance of the balanced equivalent is superior, especially as the filter memory of the FF and FB part increase. When deployed in multi-span systems, three-input partially-joint SVDFE equalizers can stretch 40 Gb/s DQPSK transmission systems beyond 800 km with very good performance and 25% lower complexity than four input joint equalization counterparts.

5. Conclusions

Optical transmission systems with phase modulation signaling combined with direct detection reception perform exceptionally well with respect to amplitude modulation formats. However their performance is dependent upon the exact configuration of the channel and the receiver choice. Especially, DQPSK formats exhibit high spectral efficiency and impairment robustness, hence, cost efficient systems could benefit from DQPSK deployment. In specific network segments, however, the cost of deployment and operation is an important issue. For that reason, constraint-limited performance evaluation is performed for all DQPSK configurations.

Typically, DQPSK receivers are either single-ended or balanced, and each case may have benefits depending on the optical channel. When electronic equalization is applied to compliment optical dispersion compensation, usually signals stemming from receivers are utilized to equalize channel dispersion. Depending on the receiver, these are either four port configurations in the case of four input single-ended receivers or a two port configuration from the balanced receiver. In this paper, starting from the requirement for low-complexity/high-performance equalizers and inspired by the need to alleviate linear dependency of the four input ports of joint single-ended equalizers and enhance numerical accuracy, the effect of reducing the number of single-ended ports in the equalization process is investigated with exceptional results. Due to the nature of DQPSK, when one destructive port is not engaged in the equalization, VDFE and low complexity SVDFE equalizers manage to compensate for residual dispersion. Especially when deployed in multi-span systems, three-port partially-joint single-ended SVDFE equalizers can exhibit exceptional performance while offering a 25% reduction in the complexity of the system with respect to the four port counterparts.

Acknowledgments: This research was supported by the Operational Program "Education and Lifelong Learning" of the Greek National Strategic Reference Framework (NSRF) Research Funding Program: THALES PROTOMI, grant number MIS 377322.

Author Contributions: M.N. designed and performed the experiments; G.G and K.G. developed and implemented the equalizers; all authors analyzed the data; all authors contributed into the writing of parts of the paper; and C.P. and G.G coordinated the overall work.

Conflicts of Interest: The authors declare no conflict of interest.

References

1. Essiambre, R.; Kramer, G.; Winzer, P.J.; Foschini, G.J.; Goebel, B.; Member, S.S. Capacity Limits of Optical Fiber Networks. *J. Light. Technol.* **2010**, *28*, 662–701. [CrossRef]
2. Nanou, M.; Politi, C.; Stavdas, A.; Glentis, G.O.; Georgoulakis, K.; Emeretlis, A.; Theodoridis, G. Cost-effective optical transponders for deployed metropolitan area networks. *Opt. Commun.* **2016**, *380*, 201–213. [CrossRef]
3. Dochhan, A.; Grießer, H.; Nadal, L.; Eiselt, M. Discrete multitone transmission for next generation 400G data center inter-connections. In Proceedings of the OptoElectronics and Communication Conference and Australian Conference on Optical Fiber Technology, Melbourne, Australia, 6–10 July 2014; pp. 3–5.
4. Lach, E.; Idler, W. Modulation formats for 100G and beyond. *Opt. Fiber Technol.* **2011**, *17*, 377–386. [CrossRef]

5. Bulow, H.; Buchali, F.; Klekamp, A. Electronic Dispersion Compensation. *J. Light. Technol.* **2008**, *26*, 158–167. [CrossRef]
6. Chen, W.; Buchali, F.; Yi, X.; Shieh, W.; Evans, J.S.; Tucker, R.S. Chromatic dispersion and PMD mitigation at 10 Gb/s using Viterbi equalization for DPSK and DQPSK modulation formats. *Opt. Express* **2007**, *15*, 5271–5276. [CrossRef] [PubMed]
7. Rosenkranz, W.; Xia, C. Electrical Equalization for Advanced Optical Communication Systems. *Int. J. Electron. Commun.* **2007**, *61*, 153–157. [CrossRef]
8. Xu, T.; Jacobsen, G.; Popov, S.; Li, J.; Vanin, E.; Wang, K.; Friberg, A.T.; Zhang, Y. Chromatic dispersion compensation in coherent transmission system using digital filters. *Opt. Express* **2010**, *18*, 16243–16257. [CrossRef] [PubMed]
9. Li, J.; Jia, J.; Zhang, L.; Zhang, F.; Chen, Z. Electrical Dispersion Compensation for 40-Gb/s DQPSK Signal Utilizing MIMO DFEs. *Photonics Technol. Lett. IEEE* **2008**, *20*, 1902–1904.
10. Nanou, M.; Emeretlis, A.; Politi, C.; Theodoridis, G.; Georgoulakis, K.; Glentis, G.O. 40 Gb/s FPGA implementation of a reduced complexity volterra DFE for DQPSK optical links. In proceesings of the 17th International Conference on Transparent Optical Networks (ICTON), Budapest, Hungary, 5–9 July 2015; pp. 1–4.
11. Glentis, G.O.; Georgoulakis, K.; Angelopoulos, K. Dispersion compensation of fiber links using pruned volterra equalizers. In Proceedings of Signal Processing in Photonics Communications (SPPCom) 2015, Boston, MA, USA, 27 June–1 July 2015.
12. Emeretlis, A.; Kefelouras, V.; Theodoridis, G.; Nanou, M.; Politi, C.; Georgoulakis, K.; Glentis, G. FPGA implementation of a MIMO DFE IN 40 GB/S DQPSK optical links. In Proceedings of the 2015 23rd European Signal Processing Conference (EUSIPCO), Nice, France, 31 August–4 September 2015; pp. 1581–1585.
13. Gorshtein, A.; Sadot, D.; Sheffi, N.; Sonkin, E.; Shachaf, Y.; Becker, D.; Levy, O.; Katz, G. Low cost 112G direct detection metro transmission system with reduced bandwidth (10G) components and MLSE compensation. *Opt. Commun.* **2015**, *338*, 438–446. [CrossRef]
14. Marsella, D.; Secondini, M.; Forestieri, E. Maximum Likelihood Sequence Detection for Mitigating Nonlinear Effects. *J. Light. Technol.* **2014**, *32*, 908–916. [CrossRef]
15. Karinou, F.; Stojanovic, N.; Goeger, G.; Xie, C.; Ortsiefer, M. 28 Gb / s NRZ-OOK Using 1530-nm VCSEL, Direct Detection and MLSE Receiver for Optical Interconnects. *Opt. Interconnects Conf.* **2015**, *5*, 20–21.
16. Nadal, L.; Svaluto Moreolo, M.; Fabrega, J. M.; Dochhan, A.; Griesser, H.; Eiselt, M.; Elbers, J.-P. DMT Modulation With Adaptive Loading for High Bit Rate Transmission Over Directly Detected Optical Channels. *J. Light. Technol.* **2014**, *32*, 4143–4153. [CrossRef]
17. Karinou, F.; Stojanovic, N.; Yu, Z. Toward Cost-Efficient 100G Metro Networks Using IMDD, 10-GHz Components, and MLSE Receiver. *J. Light. Technol.* **2015**, *33*, 4109–4117. [CrossRef]
18. Seimetz, M. *High-Order Modulation for Optical Fiber Transmission*; Springer Series in Optical Sciences; Springer Berlin Heidelberg: Berlin/Heidelberg, Germany, 2009; Vol. 143.
19. Freckmann, T.; Gonzalez, C.V.; Ruiz-Cabello Crespo, J.M. Joint Electronic Dispersion Compensation for DQPSK. In Proceedings of the Conference on Optical Fiber communication/National Fiber Optic Engineers Conference, (OFC/NFOEC 2008), San Diego, CA, USA, 24–28 February 2008; pp. 1–3.
20. Emeretlis, A.; Theodoridis, G.; Glentis, G.-O. High-performance FPGA implementations of volterra DFEs for optical fiber systems. In Proceedings of the 2014 International Conference on ReConFigurable Computing and FPGAs (ReConFig), Cancun, Mexico, 8–10 December 2014; pp. 1–8.
21. Bosco, G.; Cano, I.N.; Poggiolini, P.; Li, L.; Chen, M. MLSE-Based DQPSK Transmission in 43 ~Gb/s DWDM Long-Haul Dispersion-Managed Optical Systems. *Light. Technol. J.* **2010**, *28*, 1573–1581. [CrossRef]
22. Proakis, J. *Digital Communications*; Fourth Edi.; McGrawHill: New York, NY, USA, 2000.
23. Yadin, Y.; Orenstein, M.; Shtaif, M. Balanced versus single-ended detection of DPSK: Degraded advantage due to fiber nonlinearities. *IEEE Photonics Technol. Lett.* **2007**, *19*, 164–166. [CrossRef]
24. Wang, J.; Kahn, J.M. Impact of Chromatic and Polarization-Mode Dispersions on DPSK Systems Using Interferometric Demodulation and Direct Detection. *J. Light. Technol.* **2004**, *22*, 362–371. [CrossRef]
25. Politi, C.; Nanou, M.; Glentis, G.-O. Adaptive bit rate variable cost-effective optical networks. In Proceedings of the 2015 17th International Conference on Transparent Optical Networks (ICTON), Budapest, Hungary, 5–9 July 2015; pp. 1–4.

26. Wichmann, B.A.; Hill, I.D. Algorithm AS 183: An Efficient and Portable Pseudo-Random Number Generator. *Appl. Stat.* **1982**, *31*, 188. [CrossRef]
27. Gnauck, A.; Winzer, P.J. Optical phase-shift-keyed transmission. *Light. Technol. J.* **2005**, *23*, 115–130. [CrossRef]
28. Penninckx, D.; Bissessur, H.; Brindel, P.; Gohin, E.; Bakhti, F. Optical differential phase shift keying (DPSK) direct detection considered as a duobinary signal. *Proc. Eur. Conf. Opt. Commun.* **2001**, *3*, 456–457.
29. Chan, C.C.K. *Optical Performance Monitoring: Advanced Techniques for Next-Generation Photonic Networks*; Academic Press: Manhattan, UY, USA, 2010.
30. Alfiad, M.S.; van den Borne, D.; Hauske, F.N.; Napoli, A.; Koonen, A.M.J.; de Waardt, H. Maximum-Likelihood Sequence Estimation for Optical Phase-Shift Keyed Modulation Formats. *J. Light. Technol.* **2009**, *27*, 4583–4594. [CrossRef]